

## Possible diffusive fractionation of helium isotopes in olivine and clinopyroxene phenocrysts

DARRELL HARRISON<sup>1</sup>, TIFFANY BARRY<sup>2</sup> and GRENVILLE TURNER<sup>3</sup>

<sup>1</sup> Isotopengeologie, ETH Zentrum, Sonneggstrasse 5, CH-8092, Zurich, Switzerland  
Corresponding author, e-mail: harrison@erdw.ethz.ch

<sup>2</sup> Cardiff University (BAS/NIGL), Cardiff CF1 3YE, UK

<sup>3</sup> Department of Earth Sciences, University of Manchester, Oxford Road, Manchester M13 9PL, UK

**Abstract:** New helium isotope data ( $^3\text{He}/^4\text{He}$ ) from a series of co-genetic Siberian lavas of Cenozoic age (0.6 – 3 Ma) provide possible evidence for mass-dependent helium isotope fractionation. These lavas, erupted around the Baikal rift, have sampled sub-continental lithospheric mantle (SCLM).  $^3\text{He}/^4\text{He}$  ratios measured in clinopyroxene and olivine phenocrysts are between 0.9 – 8.3  $R_a$ . The SCLM in this region is therefore characterised by the higher unmodified  $^3\text{He}/^4\text{He}$  ratios, which are similar to the source region of mid-ocean ridge basalts (MORB). Helium isotope variation of this scale and order within local regional volcanic settings has previously been ascribed to purely, crustal contamination or radiogenic ingrowth of  $^4\text{He}$ . However, we argue that helium isotopes may also be affected by mass-dependent fractionation. This can occur during helium diffusion from the phenocrysts within sub-solidus magmas.

**Key-words:** helium isotopes; mass fractionation; diffusion; sub-continental lithospheric mantle.

### Introduction

$^3\text{He}/^4\text{He}$  isotope data are commonly used to investigate mantle sources and to constrain models of mantle and lithosphere evolution (Kellogg & Wasserburg, 1990; Dunai & Baur, 1995; Porcelli & Wasserburg, 1995; Hanyu & Kaneoka, 1997; van Keken *et al.*, 2001; Gautheron & Moreira, 2002; van Keken *et al.*, 2002; Harrison *et al.*, 2003b). A basic assumption in the use of helium isotope data is that samples have retained the helium isotope signature of their respective mantle source and/or that any processes that may have altered that signature can be recognised and modelled. There are now comprehensive helium isotope datasets available from many different regions and tectonic settings. For instance, mid-ocean ridge basalts (MORB), which are sourced in the upper mantle, are characterised by a global mean  $^3\text{He}/^4\text{He} = 8.75 R_a \pm 2.14$  ( $n = 658$ , this includes some plume-influenced ridge samples, Graham, 2002) whereas some ocean island basalts (OIB), for instance Iceland have  $^3\text{He}/^4\text{He}$  values up to  $\approx 42 R_a$  and are considered to be the product of primitive mantle plumes (Hilton *et al.*, 1999; Breddam & Kurz, 2001);  $R_a$  is the  $^3\text{He}/^4\text{He}$  ratio normalised to air, which has a value of  $1.39 \times 10^{-6}$ . Explanations for helium isotope data from MORB and OIB settings require the existence within the mantle of isolated reservoirs that have different time-integrated  $^3\text{He}/(\text{U}+\text{Th})$ , and that these reservoirs have remained isolated for periods of time long enough for different isotopic signatures to evolve.

It is also recognised however that some individual volcanic centres exhibit a large range in measured helium isotope ratios, and therefore variations in  $^3\text{He}/^4\text{He}$  do not just simply reflect differing geological settings (*i.e.* OIB vs. MORB) but also have a local control. For instance, helium isotopes measured along strike from a 12 km long fissure system on the Reykjanes Peninsula, Iceland, vary between 13 – 20  $R_a$ ; hypothesised to be the result of small-scale mantle heterogeneity (Burnard *et al.*, 2003a). Similarly large variation in  $^3\text{He}/^4\text{He}$  ratios have been recognised in the Kauai shield lavas, Hawaii (Mukhopadhyay *et al.*, 2003) and at Mauna Kea and Mauna Loa, Hawaii (Kurz *et al.*, 1996; Althaus *et al.*, 2003). Variability of  $^3\text{He}/^4\text{He}$  within a volcanic centre may reflect: (a) small-scale heterogeneity in the mantle (Burnard *et al.*, 2003a); (b) temporal and/or spatial changes as volcanic systems evolve and/or migrate with plate motion (Rison & Craig, 1983; Hilton *et al.*, 2000; Burnard *et al.*, 2003a; Mukhopadhyay *et al.*, 2003); (c) the effects of crustal-level processes, variable contamination of the source signature by assimilation of local crust or crustal fluids into the magma (crustal  $^3\text{He}/^4\text{He}$  0.01 – 0.05  $R_a$ ) (Marty *et al.*, 1994; Hilton *et al.*, 1995; Patterson *et al.*, 1997); or (d) in-growth of radiogenic  $^4\text{He}$  during crustal residence (Zindler & Hart, 1986). Alternatively, (e) experimental and theoretical evidence for helium isotope mass-dependent fractionation also exists. Several studies have previously modelled helium isotope fractionation related to helium loss through diffusion (Trull & Kurz, 1993; Dunai & Baur, 1995; Trull & Kurz, 1999).

Table 1. Sample ages and crush extraction data.

sample	age (Ma)	phase	total wt (g)	$\leq 100 \mu\text{m}$ (g)	crush fraction (%)
d-97/1	1.1 – 0.6	ol	1.12	0.10	9.4
d-97/2-2	1.1 – 0.6	ol	1.42	0.15	10.7
d-97/2-4	1.1 – 0.6	ol	1.59	0.17	10.4
d-97/3	1.1 – 0.6	ol	1.55	0.14	9.0
d-97/10-1	3.0 – 1.3	ol	0.86	0.08	9.9
d-98/27	3.0 – 1.3	ol	1.06	0.12	11.4
d-98/41	3.0 – 1.3	ol	1.19	0.11	9.6
p-536/1	1.1 – 0.6	ol	1.27	0.15	11.8
p-538/10	1.1 – 0.6	ol	1.30	0.16	12.7
d-97/1	1.1 – 0.6	cpx	1.16	0.13	11.2
d-97/2-2	1.1 – 0.6	cpx	1.16	0.17	14.6
d-97/7-2	1.1 – 0.6	cpx	0.84	0.10	12.3
d-97/9	1.1 – 0.6	cpx	0.89	0.12	13.6
d-98/27	3.0 – 1.3	cpx	1.30	0.18	13.9
d-98/59	3.0 – 1.3	cpx	1.26	0.12	9.8

In this contribution we re-evaluate and model diffusion-controlled helium isotope fractionation and within this framework we assess new helium and argon isotope data from Cenozoic basalts in southern Siberia (Tables 1 and 2). The maximum  $^3\text{He}/^4\text{He}$  ratios from these samples are similar to the mean value for the MORB source region (Graham, 2002) but the dataset contains variable and low  $^3\text{He}/^4\text{He}$  values. The region of study is clearly a continental setting with the potential for crustal contamination. We here assess the possibility that the variation in these helium isotope data is in part the result of isotope fractionation.

It is important that helium isotope systematics and the processes controlling  $^3\text{He}/^4\text{He}$  variability be fully understood in order to correctly integrate these data into geochemical and geophysical models for mantle evolution.

This manuscript forms part of an ongoing initiative by the authors and their colleagues into understanding the geological evolution of northern-central Asia. Whilst this contribution highlights the mechanisms that may cause helium isotope variation and implications thereof, a consideration of

the noble gas data within a local tectonic evolution framework will be published elsewhere.

## Geological background and samples

Throughout Asia diffuse volcanism has occurred since the Miocene (Whitford-Stark, 1987) producing small-volume alkalic basalts. A number of Cenozoic volcanic regions occur around Lake Baikal, a continental rift caused by far-field stresses associated with the collision of India with Asia. Regional geology of the area reveals that the crust is formed of accreted Palaeozoic arc terranes and micro-continental blocks. Lake Baikal is situated in a unique position within the Asian tectonic framework; northerly-flowing mantle is deflected eastwards in response to the stable Siberian craton on the northern margin of Lake Baikal. A further interest in the tectonic setting of Lake Baikal is the possibility of upwelling mantle (Petit *et al.*, 1998). We focussed on one volcanic region within the Baikal area, that of Hamar Daban, southern Lake Baikal (Fig. 1), which is sub-divided into two provinces, Dzhida and Bartoy. The region as a whole can be characterised by three phases of volcanic activity; the oldest (22 to 19 Ma) did not yield useful samples for noble gas analysis; the intermediate phase of activity (3 to 1.3 Ma) provided 4 samples which were collected from the whole of the region; and finally the youngest phase of activity (1.1 to 0.6 Ma) provided 5 samples from the Tsakir area in the south of the region (Fig. 1; age relationships from Rasskazov *et al.*, 1996). Rocks from the intermediate phase (Fig. 1) were collected from lavas between 10 and 15 m thick, which in total have an approximate volume of  $\approx 9 \text{ km}^3$ . The youngest volcanic rocks have an estimated total volume of  $\approx 2 - 2.5 \text{ km}^3$  and were erupted from three separate volcanic centres: Bartoy, Barun Hobul and Tsakir (Fig. 1). The Bartoy volcanic province is particularly noteworthy for the abundant megacrysts and mantle xenoliths that have been the subject of numerous detailed petrologic studies (Ionov *et al.*, 1992). Two further samples were selected from these mantle xenoliths.

Table 2.

sample	phase	$^4\text{He} \times 10^{-8}$	$\pm (\times 10^{-10})$	$^4\text{He}/^{20}\text{Ne}$	$^3\text{He}/^4\text{He} R_a$	$\pm$	$^3\text{He}/^4\text{He} R_c$	$^{40}\text{Ar} \times 10^{-8}$	$\pm (\times 10^{-10})$	$^{40}\text{Ar}/^{36}\text{Ar}$	$\pm$
d-97/1	ol	1.67	0.98	215.2	8.03	0.20	8.04	4.7	1.5	332.3	4.2
d-97/2-2	ol	1.34	0.79	150.0	7.99	0.20	8.00	6.2	1.9	311.2	3.3
d-97/2-4	ol	1.03	1.29	56.5	8.00	0.25	8.04	7.8	13.6	328.4	7.9
d-97/3	ol	1.22	1.49	164.6	7.96	0.28	7.98	5.5	8.1	317.2	6.9
d-97/10-1	ol	11.97	14.61	2488.4	8.12	0.25	8.12	7.8	11.5	1700.2	38.6
d-98/27	ol	0.32	0.40	128.4	7.80	0.27	7.82	3.1	5.4	532.4	15.2
d-98/41	ol	4.58	5.59	530.8	7.18	0.23	7.19	9.8	14.3	683.6	14.7
p-536/1	ol	0.12	0.16	164.2	4.73	0.31	4.74	1.5	2.4	726.4	20.7
p-538/10	ol	0.25	0.32	148.8	8.28	0.25	8.30	1.2	2.2	320.1	8.2
d-97/1	cpx	0.07	0.10	0.8	3.11	0.26	4.45	20.5	35.7	298.7	7.1
d-97/2-2	cpx	0.04	0.08	1.9	3.30	0.43	3.75	19.4	5.9	298.3	3.0
d-97/7-2	cpx	0.03	0.07	9.0	4.47	0.33	4.60	3.5	1.2	301.4	3.3
d-97/9	cpx	0.03	0.08	6.7	1.20	0.28	1.21	4.6	1.4	300.7	3.3
d-98/27	cpx	0.02	0.11	4.2	0.87	0.35	0.86	2.2	1.0	302.6	3.9
d-98/59	cpx	0.02	0.03	3.9	1.68	0.90	1.74	3.4	5.9	301.6	7.6

All gas abundances are in ml.STP. Errors are 1 sd. ol, olivine and cpx, clinopyroxene.  $R_c$  is the  $^3\text{He}/^4\text{He}$  ratio corrected for air contamination (see text).

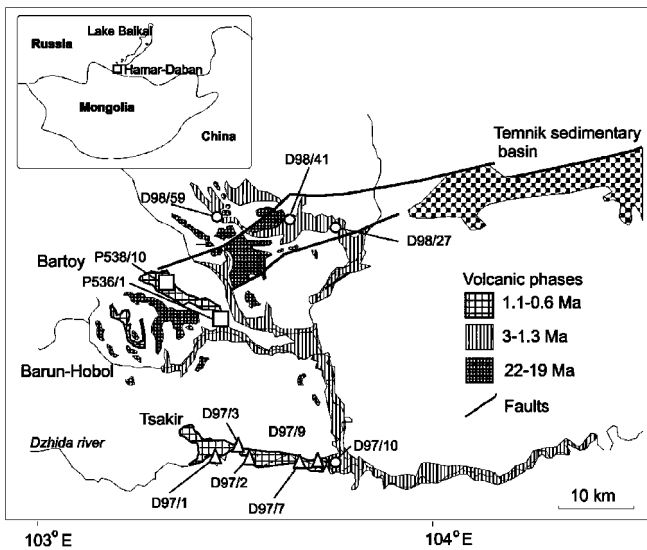


Fig. 1. Sample localities from within the Hamar-Daban volcanic province.  $\Delta$  samples from the youngest phase of volcanism (1.1 to 0.6 Ma);  $\circ$  samples from the intermediate phase of volcanism (3 to 1.3 Ma); and  $\square$  are mantle xenoliths from the Bartoy volcanic field.

## Experimental techniques for noble gas analyses

From the selected basalt samples, separates of unaltered olivine (ol) and clinopyroxene (cpx) phenocrysts (2 to 5 mm in size) were repeatedly ultrasonically cleaned with de-ionised water and finally acetone. After drying, the separates were handpicked under a binocular microscope and then loaded into a crusher system. The crusher and neighbouring sections of the stainless steel extraction line were baked at  $\leq 150$  °C under vacuum for 12 hours to liberate any adsorbed atmospheric gases prior to analysis (Burnard *et al.*, 2003b).

Helium isotope, neon abundance and argon isotope determinations were performed using the MAP 215 noble gas mass spectrometer at the University of Manchester. Gases extracted by crushing were exposed to a SAES Zr-Al getter operating at 250 °C to clean up and remove any active gases (*i.e.*  $N_2$ ,  $O_2$  and  $CO_2$ ) released during sample crushing. After purification, the gases were condensed onto an activated charcoal finger held at liquid nitrogen temperature (-196 °C). The non-condensable species, including helium, neon and  $H_2$  were then exposed to another SAES Zr-Al getter, operating at room temperature to reduce any  $H_2$  prior to introduction into the mass spectrometer. A second charcoal finger (held at -196 °C), adjacent to the source inlet valve, was used to minimise and stabilise the background levels of any residual argon,  $CO_2$  and  $H_2O$  during the helium analysis.  $^{20}Ne$  was measured during the helium run.

After helium analysis, the condensable gases were released off the charcoal finger and, prior to expansion into the mass spectrometer for argon analysis, were exposed to a room temperature SAES Zr-Al getter for secondary clean up.

$^4He$  and  $^{36,40}Ar$  isotopes were measured using a Faraday collector whilst  $^3He$  and  $^{20}Ne$  was measured using an electron multiplier in digital pulse counting mode. A resolving power of 650 on the electron multiplier at 5% of the peak

height allows for the complete separation of the  $^3He^+$  beam from any interference by the  $H_3^- - HD^+$  doublet. Noble gas abundances were calculated by peak height comparison to a known pressure of calibration gas.

Analytical blanks were determined prior to crushing steps:  $^3He$  blanks were undetectable.  $^4He$  blanks were between  $2.6 \times 10^{-12}$  and  $1.8 \times 10^{-11}$  ml.STP.  $^{20}Ne$  blanks were 1.2 to  $2.7 \times 10^{-11}$  ml.STP.  $^{40}Ar$  blanks were in the range between  $1.8 \times 10^{-10}$  and  $1.9 \times 10^{-9}$  ml.STP.

Helium concentrations (ml.STP per gram) reported in this manuscript (Table 2) were estimated using the following methodology; a similar methodology was described by Poreda & Farley, 1992. After crushing, samples were removed from the crusher system and the sample residue (crystal + powder) passed through a 100  $\mu m$  sieve: The size fraction  $> 100$   $\mu m$  (essentially powder) was carefully weighed. We assume that all gas released during crushing came from this fraction. The size fraction  $> 100$   $\mu m$  (crystal shards) still contains fluid inclusions, and is therefore considered to be essentially un-crushed material. The concentration of any volatile species = the abundance (ml.STP)  $l < 100$   $\mu m$  fraction (grams). This methodology also allows for an estimate of crushing efficiency (Table 1).

## Results

Values for  $^3He/^4He$  ratios from the Siberian samples range between 0.9 and 8.3  $R_a$  and  $^{40}Ar/^{36}Ar$  ratios vary between a near atmospheric value of  $\approx 300$  (atmospheric  $^{40}Ar/^{36}Ar = 295.5$ ) and a more radiogenic value of 1700 (Table 2). To remove any influence of atmospheric helium contamination within these analyses air contamination corrections on  $^4He$  concentration (stated as  $^4He_{corrected}$ ) have been estimated using the measured He/Ne values relative to the He/Ne value of air (X, term in eqns. 1 and 2). Atmospheric  $^3He/^4He = 1.39 \times 10^{-6}$ .

$$^4He_{corrected} = ^4He_{measured} * (X - 1) / X \quad (1)$$

Likewise, a similar correction for air contamination can be made for the measured  $^3He/^4He$  ratios (stated as  $R_c$ ).

$$^3He/^4He R_c = [(^3He/^4He R_a * X) - 1] / X - 1 \quad (2)$$

for both eqn. 1 and 2

$$X = (^4He/^{20}Ne_{measured}) / (^4He/^{20}Ne_{air}) \quad (3)$$

Most of the samples contain some atmospheric helium. However only 1 analysis requires a correction that is outside the quoted 1sd errors (Table 2). It is likely though, that the degree of atmospheric contamination in all the samples is broadly similar. However, the concentration of magmatic helium is variable and therefore the samples with less magmatic helium are more susceptible to the effects of air contamination (Harrison *et al.*, 2003a). Quoted helium concentrations and isotope ratios in the discussion have all been corrected for air contamination.

It is necessary to also consider whether post-eruption radiogenic  $^4He$  or cosmogenic  $^3He$  has affected the measured  $^3He/^4He$  ratios. We do not have strong control on the age or U and Th concentrations to stringently assess production of

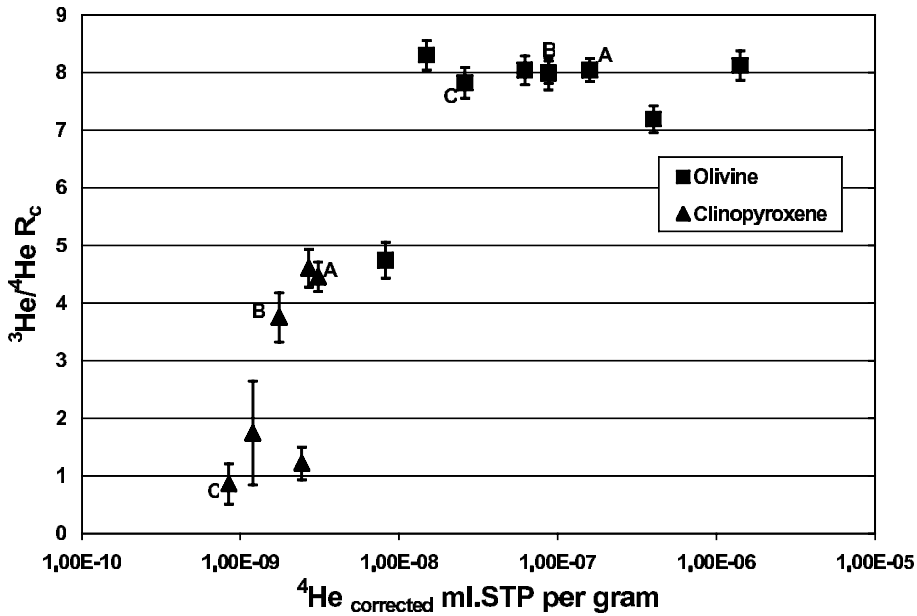


Fig. 2.  $^3\text{He}/^4\text{He } R_c$  vs.  $^4\text{He}$  concentration (corrected for air contamination). A trend of decreasing helium isotope ratio with decreasing concentration is evident. Similar trends have been observed before and ascribed to variable degrees of crustal contamination, preferentially affecting those data with most magmatic gas loss. Those samples with co-existing olivine and clinopyroxene are marked: A, d-97/1; B, d-97/2-2; C, d-98/27.

radiogenic  $^4\text{He}$ . Likewise we have little information regarding the surface exposure histories of the lavas and cannot therefore assess the production of cosmogenic  $^3\text{He}$ . It should be stated though that both of these processes produce nuclides that are sited in the crystal matrix. Importantly, all the analyses were performed using a pressure fracturing mechanism to release volatiles from the samples. Pressure fracturing crushers are designed to release volatiles from fluid inclusions and not matrix-sited volatiles. Only a single crushing step was performed on each sample and the percentage of sample actually crushed is of the order 10% (Table 1). This degree of crushing is highly unlikely to release any significant amounts of matrix-sited gases (Scarsi, 2000). The helium measured can therefore be considered representative of the fluid inclusions hosted by the phenocrysts.

$^3\text{He}/^4\text{He } R_c$  is plotted against helium concentration in Fig. 2. The correlation (decreasing  $^3\text{He}/^4\text{He}$  with decreasing concentration) and isotopic disequilibria between co-existing olivine and clinopyroxene phases is not uncommon in basalt datasets (Marty *et al.*, 1994; Hilton *et al.*, 1995). This has previously been attributed to variable amounts of a crustally derived  $^4\text{He}$  contaminant ( $^3\text{He}/^4\text{He}$  0.01 – 0.05  $R_a$ ) admixed into a degassing magma or in-growth of radiogenic  $^4\text{He}$  within the magma, over time-scales sufficient to allow isotopic exchange. The above hypothesis implies that the commonly lower  $^3\text{He}/^4\text{He}$  ratios found in clinopyroxene compared to olivine may be broadly interpreted in two ways:

1. Clinopyroxene postdates olivine and has therefore trapped helium at a later date within a parent magma with a decreasing  $^3\text{He}/^4\text{He}$  ratio or,

2. Lower  $^3\text{He}/^4\text{He}$  ratios in clinopyroxene may be the result of a lower effective closure temperature. Clinopyroxene will continue to exchange helium with the magma after the olivine had become closed (Marty *et al.*, 1994; Hilton *et al.*, 1995).

A time-dependent decrease of  $^3\text{He}/^4\text{He}$  within magma has previously been used to explain helium isotope varia-

tions at Heard Island in the Indian Ocean (Hilton *et al.*, 1995) and the Tabar-Lihir-Tanga-Feni island arc, Papua New Guinea (Patterson *et al.*, 1997) amongst others.

However as we suggest below, the samples described in this paper appear to have originally trapped noble gases, whose elemental ratios (He/Ar) are inconsistent with being trapped in a degassing, ageing magma. We present a simple theoretical model describing helium isotope fractionation caused through a vacancy diffusion mechanism. This model is then applied to new data in order to assess the possibility that isotope fractionation may affect natural samples.

## Discussion

### Diffusive fractionation of helium isotopes

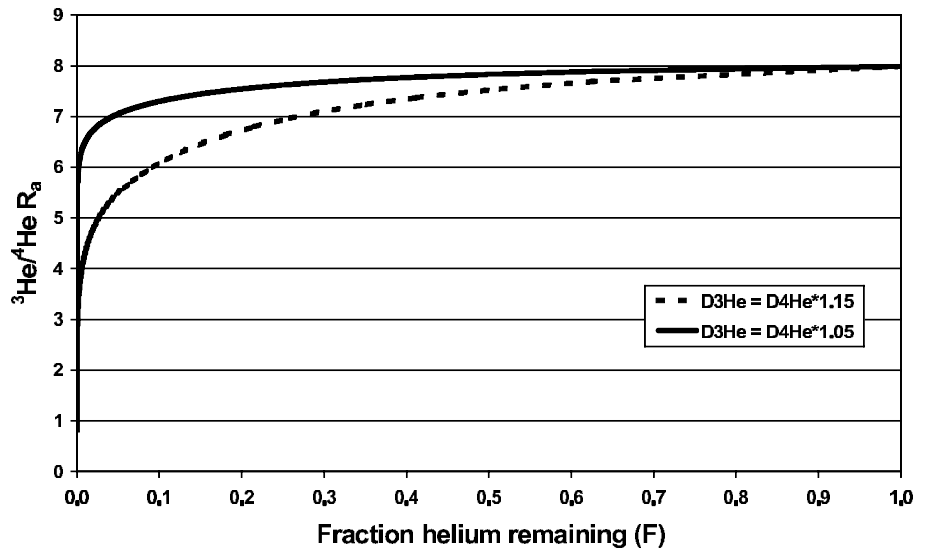
Helium is dominantly sited in  $\text{CO}_2$ -rich fluid inclusions in olivine and pyroxene phenocrysts. Any helium loss from the crystals must therefore involve several processes. These are helium solution at the inclusion-crystal boundary, diffusion through the crystal lattice (also along micro-fractures) and then desorption from the crystal surface. Within the crystal volume the rate is controlled by the diffusivity and the quantity by the helium solubility. The modelling presented here assumes homogenous initial helium distribution and does not implicitly consider fluid inclusion densities and helium solution between inclusion and grain. This approach has been used previously to calculate actual diffusivities (Trull & Kurz, 1993) and has the advantage that the mathematics and computations are simple.

The relative mass difference between  $^3\text{He}$  and  $^4\text{He}$  is large. Predicted differences in their diffusivities should therefore be significant and can be defined by the following,

$$(D_{^3\text{He}}/D_{^4\text{He}}) - 1 = (M_{^4\text{He}}/M_{^3\text{He}})^{1/2} - 1 \quad (4)$$

D is the diffusivity and M is the relative atomic mass.

Fig. 3.  ${}^3\text{He}/{}^4\text{He}$   $R_a$  vs.  $F$  (theoretical modelling). The relative mass difference between  ${}^3\text{He}$  and  ${}^4\text{He}$  is large. Solid-state diffusion and gas laws predict that differences in their diffusivities should be significant. It is possible therefore that fractionation of helium isotopes may occur within phenocrysts during storage within sub-solidus magmas. This modelling assumes a spherical grain, with a uniform initial concentration and a constant surface concentration. Two runs have been computed and we have assumed a constant diffusivity for  ${}^4\text{He}$  ( $D^4\text{He}$ ).  ${}^3\text{He}$  diffusivity has been calculated as  $D^4\text{He} * 1.15$  and  $D^4\text{He} * 1.05$  (15% and 5% faster than  ${}^4\text{He}$ ).



Equation 4 describes the inverse square root of mass relationship assuming vacancy diffusion mechanisms, as applicable to noble gases (Trull & Kurz, 1999).  ${}^3\text{He}$  should therefore diffuse 15% faster than  ${}^4\text{He}$ . This is broadly consistent with experimentally determined  ${}^3\text{He}$  and  ${}^4\text{He}$  diffusivities in olivine and basalt glass (Trull & Kurz, 1993, 1999). It is possible therefore that fractionation of helium isotopes may occur within phenocrysts during storage within sub-solidus magmas. We have produced a simple model to assess this possibility.

Assuming a spherical grain, with a uniform initial concentration and if the surface concentration is maintained constant the following equation can be written (Crank, 1975),

$$\frac{C - C_i}{C_o - C_i} = 1 + \frac{2a}{\pi} \sum_{n=1}^{\infty} \frac{(-1)^n}{n} \sin \frac{n\pi r}{a} \exp\left(-\frac{Dn^2\pi^2 t}{a^2}\right) \quad (5)$$

$C$  = concentration,  $C_i$  = initial concentration,  $C_o$  = surface concentration,  $D$  = diffusivity,  $t$  = time therefore,

$$C = \left[ 1 + \frac{2a}{\pi} \sum_{n=1}^{\infty} \frac{(-1)^n}{n} \sin \frac{n\pi r}{a} \exp\left(-\frac{Dn^2\pi^2 t}{a^2}\right) \right] (C_o - C_i) + C_i \quad (6)$$

integrating for  $C$  over the volume (average  $C(t)$ ),

$$\bar{C} = C_o + \frac{6C_o X}{\pi^3} - \frac{6C_i X}{\pi^3} \quad (7)$$

where,

$$X = \sum_{n=1}^{\infty} \left( -\frac{(-1)^n \pi \cos(n\pi)}{en^2} + \frac{(-1)^n \pi \sin(n\pi)}{en^3} \right) \quad (8)$$

and

$$e = \exp\left(-\frac{Dn^2\pi^2 t}{a^2}\right) \quad (9)$$

Fig. 3 ( ${}^3\text{He}/{}^4\text{He}$  vs.  $F$ , fraction of helium remaining in the phenocryst) shows theoretical results of two computations

using equation 7. Both runs have assumed a constant diffusivity for  ${}^4\text{He}$  ( $D^4\text{He}$ ).  ${}^3\text{He}$  diffusivity has been calculated as  $D^4\text{He} * 1.15$  and  $D^4\text{He} * 1.05$  (15% and 5% faster than  ${}^4\text{He}$ ) to allow for variation in actual relative diffusivity; 15% to model the inverse square root of mass relationship and 5% to approximate previously measured values (Trull & Kurz, 1999). It has been suggested that diffusivity may have temperature dependence (lower relative rates at lower temperatures) (Trull & Kurz, 1999). The actual  $D^4\text{He}$  used in the model is not important, as Fig. 3 is not rate-dependent. However assuming a 5 mm radius grain and  $D^3\text{He}$  of both  $D^4\text{He} * 1.15$  and  $D^4\text{He} * 1.05$  ( $D^4\text{He} = 1.5 \times 10^{-10} \text{ cm}^2 \text{ s}^{-1}$  in olivine at  $1400^\circ\text{C}$ , Trull & Kurz, 1993) the  ${}^3\text{He}/{}^4\text{He}$  ratio will drop from 8 to 4  $R_a$  after approximately 60 and 180 years respectively. The rate of change is highly dependent on the radius of the grain (see equation 9). For a 2 mm radius grain these rates change to approximately 2 and 6 years respectively. Irrespective of the actual rate of change, the important aspect of Fig. 3 is the  $F$  value for any given  ${}^3\text{He}/{}^4\text{He}$  ratio. Assuming  ${}^3\text{He}$  is 15% faster than  ${}^4\text{He}$ ,  ${}^3\text{He}/{}^4\text{He}$  ratios of 5 and 2  $R_a$  equate to  $F$  values  $\approx 0.03$  and  $\approx 0.00006$  respectively. An  $F$  value of  $\approx 0.00006$  implies the grain will have lost  $\approx 99.994\%$  of its initial helium budget.

Testing this hypothesis for natural data requires a methodology by which to calculate an  $F$  value for any given sample. This is problematic because noble gases may be lost during degassing of a melt and initial concentrations of helium will vary between samples. However degassing of a silicate melt also fractionates noble gas elemental ratios according to their relative solubilities (solubility decreases with increasing atomic mass) (Lux, 1987; Carroll & Draper, 1994). It is possible to predict the likely  ${}^4\text{He}/{}^{40}\text{Ar}^*$  radiogenic production ratio in a magma source region based on estimates of mantle K, U, and Th compositions (superscript “\*”, corrected for atmospheric  ${}^{40}\text{Ar}$  contribution). These predicted ratios are used to quantify the degree of fractionation (equilibrium or kinetic) in any given analysis, provided the production ratios are constant. For instance a mantle reservoir isolated for 4 Ga will have an accumulated  ${}^4\text{He}/$

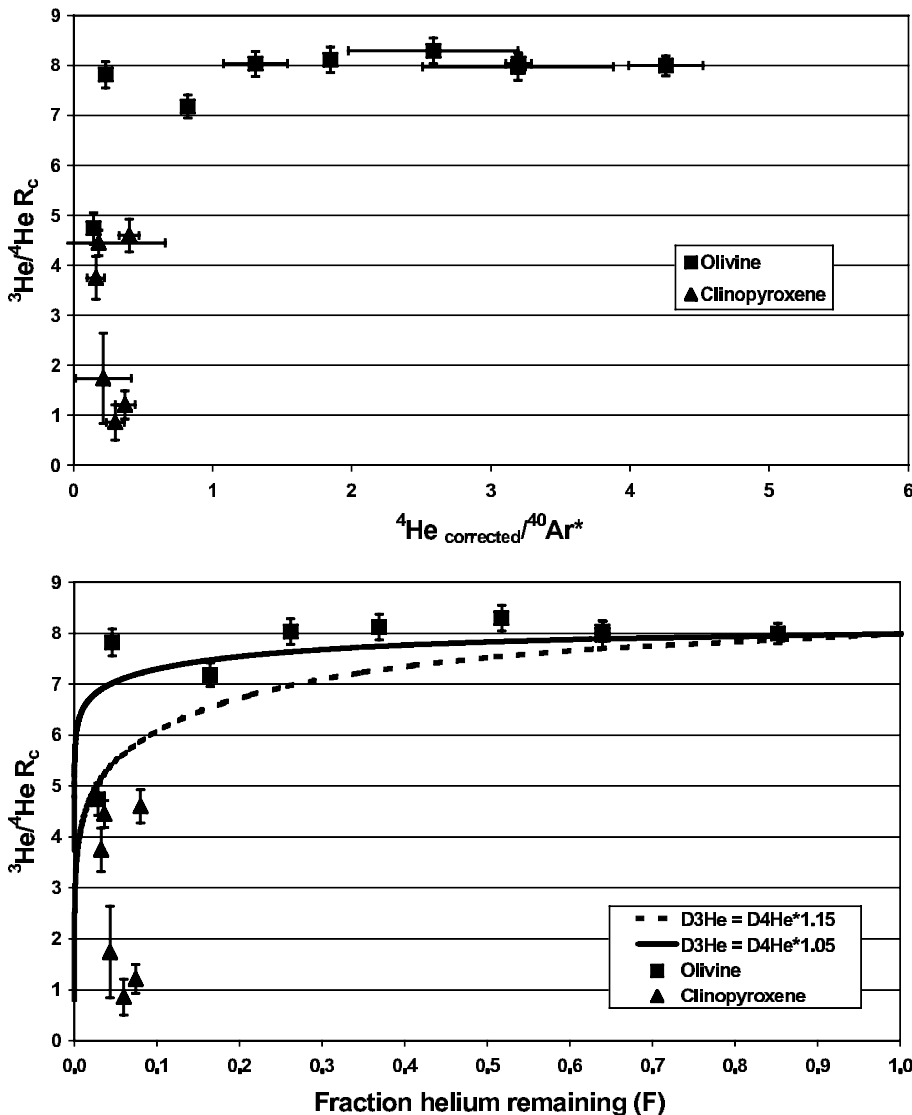


Fig. 4.  $^3\text{He}/^4\text{He} R_c$  vs.  $^4\text{He}_{\text{corrected}}/^{40}\text{Ar}^*$ . Assuming that only helium loss has occurred we can estimate the degree of helium loss by reference to the elemental fractionation index,  $^4\text{He}/^{40}\text{Ar}^*$ . Variable  $^4\text{He}/^{40}\text{Ar}^*$  ratios can be produced by solubility controlled degassing processes. However helium is more soluble than argon in a silicate melt, therefore, solubility controlled fractionation cannot produce lower ratios than the presumed mantle production value of  $\approx 5$ . The variable but low  $^4\text{He}/^{40}\text{Ar}^*$  values can be explained by helium loss from the phenocrysts after volatile trapping, and during residence in magma prior to eruption.

Fig. 5.  $^3\text{He}/^4\text{He} R_c$  vs. F (theoretical and new data). Comparison of theoretical modelling from Fig. 3 with Siberian data. F values for these data estimated using the following equation,  $F = (^4\text{He}/^{40}\text{Ar}^*_{\text{measured}}) / (^4\text{He}/^{40}\text{Ar}^*_{\text{initial}})$ . Excess  $^{40}\text{Ar}$  ( $^{40}\text{Ar}^*$ ) is calculated as,  $^{40}\text{Ar}^* = ^{40}\text{Ar} - (^{36}\text{Ar} * 295.5)$ . A number of the analyses, particularly the clinopyroxenes, have near-atmospheric  $^{40}\text{Ar}/^{36}\text{Ar}$  values (atmospheric  $^{40}\text{Ar}/^{36}\text{Ar} = 295.5$ ). Therefore  $^{40}\text{Ar}^*$  values may be small. Estimated  $^4\text{He}/^{40}\text{Ar}^*$  values (and therefore the F values) are accurate but uncertainties may be large. Errors for F values not shown.

$^{40}\text{Ar}^*$  of  $\approx 2$  ( $K/U = 12,700$ ,  $\text{Th}/U = 2.6$ ), whereas a 1 Ga isolation period will result in an accumulated  $^4\text{He}/^{40}\text{Ar}^*$  of  $\approx 4$  and an instantaneous  $^4\text{He}/^{40}\text{Ar}^*$  production ratio  $\approx 5$ , for the same  $K/U$  and  $\text{Th}/U$  (Allègre *et al.*, 1986; Burnard *et al.*, 1997). Because argon is less soluble than helium in a silicate melt, if that melt undergoes degassing the  $^4\text{He}/^{40}\text{Ar}^*$  value in the residual melt will increase, as argon is preferentially partitioned into the vapour phase. If we consider the Siberian data, the maximum  $^4\text{He}/^{40}\text{Ar}^*$  value is  $\approx 4$  with all other data variable but low (Fig. 4). Assuming an initial  $^4\text{He}/^{40}\text{Ar}^*$  in the melt of 5 (instantaneous production value), this trend cannot be due to solubility controlled degassing (*i.e.* the samples will have trapped noble gases with variable but high  $\text{He}/\text{Ar}$  ratios in a degassing magma). Instead it seems likely that these phenocryst samples trapped relatively unfractionated noble gases in magma. The variable but low  $^4\text{He}/^{40}\text{Ar}^*$  values can then be explained by helium loss from the phenocrysts after volatile trapping, and during residence in magma prior to eruption. This is further supported by the broad correlation between low  $^4\text{He}/^{40}\text{Ar}^*$  ratios and low  $^4\text{He}$  concentration.

As a first order approximation, taking a  $^4\text{He}/^{40}\text{Ar}^*$  value of 5 as the initial trapped ratio in the magma and assuming only helium loss to have occurred we can estimate an F value for helium for any given sample. If clinopyroxene post-dates olivine they may have trapped noble gases with a  $^4\text{He}/^{40}\text{Ar}^*$  ratio  $> 5$ . Nevertheless, the subsequent degree of helium loss to produce  $^4\text{He}/^{40}\text{Ar}^*$  ratios  $< 0.4$  is high, therefore estimated F values  $< 0.1$  are not overly sensitive relative to the exact initial  $^4\text{He}/^{40}\text{Ar}^*$  used.

$$F = (^4\text{He}/^{40}\text{Ar}^*_{\text{measured}}) / (^4\text{He}/^{40}\text{Ar}^*_{\text{initial}}) \quad (10)$$

F values for the new Siberian data have been estimated and the results plotted in Fig. 5. The olivine and one sub-group of the clinopyroxene data are in broad agreement with the theoretical modelling (Fig. 3). However, three clinopyroxene analyses with  $^3\text{He}/^4\text{He}$  values  $< 2 R_c$  do not concur with the modelled fractionation curves. As previously stated, to theoretically produce a  $^3\text{He}/^4\text{He}$  value  $\approx 2 R_a$  by diffusive fractionation requires that the grain has lost  $\approx 99.994\%$  of its initial helium budget (assuming  $D^3\text{He} = D^4\text{He} * 1.15$ ). These clinopyroxenes have F values that equate to losses of the or-

der 95%. As a consequence the “excess”  $^4\text{He}$  is likely to have been derived from the local crust and has overprinted any possible effect from fractionation, although determining the relative importance of either process is not possible at the moment.

## Implications and conclusions

Helium isotope data from OIB and continental settings are an integral part of many mantle evolution models. Estimated mean  $^3\text{He}/^4\text{He}$  values, from a particular tectonic setting, are often used in such models. Low helium concentration  $^3\text{He}/^4\text{He}$  analyses appear to be prevalent in OIB and continental settings. If we assume that extensive helium loss equates with a lowered  $^3\text{He}/^4\text{He}$  ratio (whether due to fractionation or crustal contamination) then a significant proportion of any compiled dataset could be discarded. This could lead to higher estimates of the mean  $^3\text{He}/^4\text{He}$  ratio and thus to a degree invalidate the original modelling. However, irrespective of the statistics involved in calculating helium isotope mean values, it may be prudent to instead carefully assess the highest measured  $^3\text{He}/^4\text{He}$  from a particular setting as being more representative of the source rather than an estimated mean value (assuming a single value can represent the source and also with or without filtering the low concentration data). For the sub-continental lithospheric mantle in the Lake Baikal region of Siberia this equates to a MORB-like helium isotope signature.

**Acknowledgements:** DH would like to thank everybody in the Manchester Cosmochemistry and Geochemistry group for showing a great deal of patience and their friendship during his stay there. DH would also like to thank G. Simpson at ETH for introducing me to Crank. TB says thanks to S. Rasskazov, A. Ivanov and L. Demonerova for geological know-how and samples. We thank M. Trieloff and an anonymous reviewer for thoughtful and helpful comments.

## References

- Allègre, C. J., Staudacher, T. *et al.* (1986): Rare gas systematics: formation of the atmosphere, evolution and structure of the Earth's mantle. *Earth Planet. Sci. Lett.*, **87**, 127-150.
- Althaus, T., Niedermann, S., Erzinger, J. (2003): Noble gases in olivine phenocrysts from drill core samples of the HSDP pilot and main holes (Mauna Loa and Mauna Kea, Hawaii). *Geochem. Geophys. Geosys.*, 2001GC000275.
- Breddam, K. & Kurz, M. D. (2001): Helium isotopic signatures of Icelandic alkaline lavas. *Eos*, **82**(47).
- Burnard, P., Harrison, D. *et al.*, (2003a): Argon isotope constraints on modification of oxygen isotopes by surficial processes. *Chemical Geol.*, *subm.*
- , – *et al.* (2003b): The degassing and contamination of noble gases in mid-Atlantic Ridge basalts. *Geochem. Geophys. Geosys.*, **4**(1).
- Burnard, P. G., Graham, D. W. *et al.* (1997): Vesicle-specific noble gas analyses of “popping rock”: implications for primordial noble gases in the Earth. *Science*, **276**, 568-571.
- Carroll, M. R. & Draper, D. S. (1994): Noble gases as trace elements in magmatic processes. *Chemical Geol.*, **117**(1-4), 37-56.
- Crank, J. (1975): *The Mathematics of Diffusion*. Oxford Science Publications. Equation 6.18, p. 91.
- Dunai, T. J. & Baur, H. (1995): Helium, neon and argon systematics of the European subcontinental mantle: Implications for its geochemical evolution. *Geochim. Cosmochim. Acta*, **59**, 2767-2783.
- Gautheron, C. & Moreira, M. (2002): Helium signature of the sub-continental lithospheric mantle. *Earth Planet. Sci. Lett.*, **199**, 39-47.
- Graham, D. W. (2002): Noble gas isotope geochemistry of mid-ocean ridge and ocean island basalts: Characterization of mantle source reservoirs. *Rev. Min. Geochem.*, **47**, 247-318.
- Hanyu, T. & Kaneoka, I. (1997): The uniform and low  $^3\text{He}/^4\text{He}$  ratios of HIMU basalts as evidence for their origin as recycled materials. *Nature*, **390**, 273-276.
- Harrison, D., Burnard, P. G. *et al.*, (2003a): Resolving atmospheric contaminants in mantle noble gas analyses. *Geochem. Geophys. Geosys.*, **4**(3).
- Harrison, D., Leat, P. T. *et al.*, (2003b): Resolving mantle components in oceanic lavas from segment E2 of the East Scotia Back-Arc Ridge. *J. Geol. Soc. London, Spec. Publ.* **219**, 333-344.
- Hilton, D. R., Barling, J. *et al.*, (1995): Effect of shallow-level contamination on the helium isotope systematics of ocean-island lavas. *Nature*, **373**, 330-333.
- Hilton, D. R., Gronvold, K. *et al.*, (1999): Extreme He-3/He-4 ratios in northwest Iceland: constraining the common component in mantle plumes. *Earth Planet. Sci. Lett.*, **173**, 53-60.
- Hilton, D. R., Macpherson, C. G. *et al.*, (2000): Helium isotope ratios in mafic phenocrysts and geothermal fluids from La Palma, the Canary Islands (Spain): Implications for HIMU mantle sources. *Geochim. Cosmochim. Acta*, **64**, 2119-2132.
- Ionov, D. A., Kramm, U. *et al.*, (1992): Evolution of the upper mantle beneath the southern Baikal rift zone: an Sr-Nd isotope study of xenoliths from the Bartoy volcanoes. *Contrib. Mineral. Petrol.*, **111**, 235-247.
- Kellogg, L. H. & Wasserburg, G. J. (1990): The role of plumes in mantle He fluxes. *Earth Planet. Sci. Lett.*, **99**, 276-789.
- Kurz, M. A., Kenna, T. C., Lassiter, J. C., DePaolo, D. J. (1996): Helium isotope evolution of Mauna Kea volcano: First results from the 1-km drill core. *J. Geophys. Res.*, **101**, 11769-11780.
- Lux, G. (1987): The behaviour of noble gases in silicate liquids: solution, diffusion, bubbles and surface effects, with applications to natural samples. *Geochim. Cosmochim. Acta*, **51**, 1549-1560.
- Marty, B., Trull, T. *et al.*, (1994): He, Ar, O, Sr and Nd isotope constraints on the origin and evolution of Mount Etna magmatism. *Earth Planet. Sci. Lett.*, **126**, 23-39.
- Mukhopadhyay, S., Lassiter, J. C. *et al.*, (2003): Geochemistry of Kauai shield-stage lavas: implications for the chemical evolution of the Hawaiian plume. *Geochem. Geophys. Geosys.*, **4**(1).
- Patterson, D. B., Farley, K. A. *et al.*, (1997): Helium Isotopic Composition Of the Tabar Lihir Tanga Feni Island Arc, Papua New Guinea. *Geochim. Cosmochim. Acta*, **61**, 2485-2496.
- Petit, C., Koulakov, I. *et al.*, (1998): Velocity structure around the Baikal rift zone from teleseismic and local earthquake travel-times and geodynamic implications. *Tectonophysics*, **296**, 125-144.
- Porcelli, D. & Wasserburg, G. J. (1995): Mass transfer of helium, neon, argon, and xenon through a steady-state upper mantle. *Geochim. Cosmochim. Acta*, **59**, 4921-4937.
- Poreda, R. J. & Farley, K. A. (1992): Rare Gases in Samoan Xenoliths. *Earth Planet. Sci. Lett.*, **113**, 129-144.
- Rasskazov, S. V., Kunk, M. J. *et al.*, (1996): Episodes of eruptions and compositional variations of the Quaternary lavas in the Baikal rift system. *Russ. Geol. Geophys.*, **37**, 1-12.

- Rison, W. & Craig, H. (1983): Helium isotopes and mantle volatiles in Loihi Seamount and Hawaiian Island basalts and xenoliths. *Earth Planet. Sci. Lett.*, **66**, 407-426.
- Scarsi, P. (2000): Fractional extraction of helium by crushing of olivine and clinopyroxene phenocrysts: effects on the  $^3\text{He}/^4\text{He}$  measured ratio. *Geochim. Cosmochim. Acta*, **64**, 3751-3762.
- Trull, T. & Kurz, M. D. (1993): Experimental measurements of  $^3\text{He}$  and  $^4\text{He}$  mobility in olivine and clinopyroxene at magmatic temperatures. *Geochim. Cosmochim. Acta*, **47**: 1313-1324.
- , – (1999): Isotopic fractionation accompanying helium diffusion in basaltic glass. *J. Molecular Structure*, **485-486**, 555-567.
- van Keken, P. E., Ballentine, C. J. *et al.*, (2001): A dynamical investigation of the heat and helium imbalance. *Earth Planet. Sci. Lett.*, **188**, 421-434.
- van Keken, P. E., Hauri, E. *et al.*, (2002): Mantle mixing: the generation, preservation, and destruction of chemical heterogeneity. *Ann. Rev. Earth Planet. Sci.*, **30**, 11.1-11.33.
- Whitford-Stark, J. L. (1987): A survey of Cenozoic volcanism on mainland Asia. *Geol. Soc. Amer. Spec. Pap.*, **213**, 74 p.
- Zindler, A. & Hart, S. R. (1986): Helium: problematic primordial signals. *Earth Planet. Sci. Lett.*, **79**: 1-8.

*Received 20 June 2003*

*Modified version received 14 October 2003*

*Accepted 1 December 2003*